

TRPA1 is a substrate for de-ubiquitination by the tumor suppressor CYLD

Alexander Stokes^a, Clay Wakano^a, Murielle Koblan-Huberson^a, Chaker N. Adra^{c,d},
Andrea Fleig^b, Helen Turner^{a,*}

^a *Laboratory of Cell Biology and Immunology, Center for Biomedical Research at Queen's Medical Center, Honolulu, HI, USA*

^b *Laboratory of Cell and Molecular Signaling, Center for Biomedical Research at Queen's Medical Center, Honolulu, HI, USA*

^c *Harvard Medical School, Department of Medicine and Department of Pathology, Hematology/Oncology Division,
Beth Israel Deaconess Medical Center, Boston, MA, USA*

^d *Department of Medicine, Division of Nephrology, Transplantation Center, The Children's Hospital, Boston, MA, USA*

Received 11 November 2005; received in revised form 24 December 2005; accepted 26 December 2005

Available online 23 February 2006

Abstract

Certain TRP cation channels confer the ability to sense environmental stimuli (heat, cold, pressure, osmolarity) across physiological and pathophysiological ranges. TRPA1 is a TRP-related channel that responds to cold temperatures, and pungent compounds that include the cold-mimetic icilin and cannabinoids. The initial report of TRPA1 as a transformation-associated gene product in lung epithelia is at odds with subsequent descriptions of a tissue distribution for TRPA1 that is restricted to sensory neurons. Here, we report that the human TRPA1 protein is widely expressed outside the CNS, and is indeed dys-regulated during oncogenic transformation. We describe that TRPA1 associates with the tumor-suppressor protein CYLD. TRPA1 is a novel substrate for the de-ubiquitinating activity of CYLD, and this de-ubiquitination has the net effect of increasing the cellular pool of TRPA1 proteins. Oncogenic mutations in the *CYLD* gene may therefore be predicted to alter cellular levels of TRPA1.

© 2006 Elsevier Inc. All rights reserved.

Keywords: TRPA1; CYLD; Ubiquitination; Cylindroma; Icilin

1. Introduction

TRPA1 is a calcium-permeant cation channel that has been implicated in the cellular sensing of physical stimuli (cold temperatures and mechanical stress), and chemical stimuli that include cannabinoids and pungent compounds [1–7]. TRPA1 has a physiological role in sensory neurons, but the newly described diversity in its activation mechanisms suggests that the channel may mediate responses in non-neuronal cell types. Indeed, the original description of TRPA1 (ANKTM1) was made in lung fibroblasts, where a link between oncogenic transformation status and dys-regulation of TRPA1 expression levels was also postulated [8,9]. Mechanisms that control expression levels of TRPA1, or those of related TRP channels, are poorly understood, but may be important for our

understanding of both physiological, and pathophysiological, roles for these ion channels.

Post-translational processes are recognized as key determinants of the expression levels of numerous proteins. Two major pathways effect control at this level, comprising cysteine-directed proteases (the lysosomal cathepsins and cytoplasmic calpains), and the 26 S proteasome complex [10–13]. Ubiquitination (reversible addition of the 76 amino acid/8.5 kDa ubiquitin molecule) of proteins plays an important initiating role in the latter process, since poly-ubiquitination of a protein precedes its degradation by the proteasome complex [13–15]. Ubiquitination is a highly regulated process, and extensive classes of pro-ubiquitination (ubiquitin ligases), and de-ubiquitinating (ubiquitin hydrolases) enzymes have been described [13,16]. Given the centrality of these enzymes in controlling protein lifetime, it is perhaps unsurprising that several oncogene and tumor suppressor gene products are components of the ubiquitination machinery [10,13]. For example, the product of the *CYLD* tumor suppressor gene is a ubiquitin hydrolase [17–20], and heritable loss-of-function

* Corresponding author. Queen's Medical Center, University Tower 811, 1356 Lusitana Street, Honolulu, HI 96813, USA. Tel.: +1 808 537 7927; fax: +1 808 537 7926.

E-mail address: hturner@queens.org (H. Turner).

mutations in the CYLD protein are associated with the development of cylindromas, trichoepitheliomas, and adenoid cystic carcinomas [21–27]. As for many members of the ubiquitination machinery, the full complement of targets for CYLD activity has not yet been elucidated.

Ubiquitination is used as a method of signal termination, and signal modulation, for some plasma membrane receptors and ion channels [14,15,28]. Examples of the ubiquitin degradation system regulating cell surface receptors include growth factor [29–31] and antigen receptors [32–34]. Ubiquitination may follow ligand binding to the receptor, and hence can be component of the signal termination mechanism [14,32,34,35]. Ubiquitination of receptors can lead to protein degradation via the proteasome, but may also initiate endocytosis and targeting for degradation via the lysosome. In this latter pathway, ubiquitination may not be the only commitment step for protein degradation, since de-ubiquitination and recycling of protein to the plasma membrane have been described. In this case, ubiquitination following receptor ligation may be part of a staging process that precedes recycling to the cell surface. Similar mechanisms are likely to operate for ion channels, although the literature on regulated ubiquitination of this class of proteins is less extensive. Previous studies indicate that levels of aquaporin water channels are upregulated in response to hypo-osmotic conditions via a decrease in the ubiquitination status of the channel proteins [36,37]. Similarly, sodium channels of the ENaC class are regulated by the Nedd ubiquitin ligases, which in turn respond to both acute, and developmental, signals [38–41]. A role for ubiquitination in either ligand responsiveness, or basal expression control, of TRP channels has not previously been explored.

Here, we report a post-translational mechanism for control of TRPA1 protein levels. The initial report of TRPA1 as a transformation-associated gene product in lung epithelia [8] is at odds with subsequent descriptions of a tissue distribution for TRPA1 that is restricted to sensory neurons [1–3]. Here we report that the human TRPA1 protein is widely expressed outside the CNS, and changes in TRPA1 protein levels are associated with transformed phenotypes. On the basis of these findings, it was proposed that TRPA1 levels could be controlled via regulation of channel protein lifetime—an aspect not previously investigated for the TRPA1 channel. Data are presented that suggest a potential post-translational mechanism for control of TRPA1 protein levels by the product of a novel human tumor suppressor gene, *CYLD*. TRPA1 is a novel substrate for the de-ubiquitinating activity of the *CYLD* enzyme, and this de-ubiquitination causes a net increase in the cellular pool of TRPA1 proteins. Oncogenic mutations in *CYLD* would be predicted to alter the expression levels of TRPA1.

2. Materials and methods

2.1. Maintenance of cell cultures

HEK293 stably transfected with pcDNA6TR (Invitrogen, CA), were maintained in DMEM/10% fetal bovine serum/2 mM glutamine in humidified 5% CO₂ at 37 °C. All other cell lines were maintained in appropriate culture media under the same incubation conditions.

2.2. Production of inducible stable cell lines

The HEK293T-REx™ Cell Line stably expresses the tetracycline repressor protein (Invitrogen, Carlsbad, CA). TReX-based cell lines exhibit low basal expression of the protein of interest in the repressed state and high expression upon treatment with tetracycline. For production of TReX HEK293 cells with inducible expression of TRPA1, parental cells were electroporated with 15 µg of plasmid DNA in a 500 µl volume of DMEM/10% FBS/2 mM Gln. Electroporations were performed at 280 V/950 µF in a 4 mm path length cuvette (BioRad, Hercules, CA). Clonal cell lines were selected by limiting dilution in 400 µg/ml hygromycin (Invitrogen, CA), and screened by immunoprecipitation and Western blot. Transfected gene expression was induced using 1 µg/ml tetracycline for 16 h at 37 °C.

2.3. Transient transfection

HEK293TReX cells (Invitrogen, Carlsbad, CA) were seeded and grown until 50% confluent. All cDNA was purified using a QIAfilter Plasmid Maxi Kit (Qiagen, Valencia, CA). The cDNA quality was measured using a spectrophotometer and used in transfection only if O.D. 260/280 > 1.7. HEK293 cells were transiently transfected using reagent LT1 (Mirus, Madison, WI). Serum free DMEM (100 µl) and LT1 reagent (10 µl) were added together and vortexed for 30 s. The mixture was then left at room temperature for 15 min. After 15 min, the cDNA was added to the mixture and mixed gently. After 15 min at RT, the mixture was added to the cells in a drop-wise manner while swirling the plate. The cells were then placed in a humidified 5% CO₂ incubator for 48–72 h. The cells were then harvested and lysed as described above.

2.4. Immunoprecipitation and Western blot

Cells were pelleted (2000 g, 2 min) and washed once in ice cold PBS. Approximately 10⁷ cells were lysed (ice/30 min) in 350 µl of lysis buffer (50 mM Hepes pH 7.4, 75 mM NaCl, 20 mM NaF, 10 mM iodoacetamide, 0.5% (w/v) Triton X100, 1 mM PMSF (phenylmethylsulfonyl fluoride), 500 µg/ml Aprotinin, 1.0 mg/ml Leupeptin and 2.0 mg/ml chymostatin). Lysates were then clarified (10,000 g, 5 min). For preparation of total protein, lysates were acetone precipitated. For immunoprecipitation, supernatants were tumbled (4 °C/2 h) with the indicated antibody, covalently coupled (dimethylpimelidate/ethanolamine) to Protein A sepharose. Samples were boiled in reducing sample buffer (20% (v/v) glycerol, 62.5 mM Tris-HCl pH 6.8, 0.05% (w/v) bromophenol blue, 2 mM 2mercapto-ethanol), resolved by SDS-PAGE, and electro-transferred to Polyvinylidene Fluoride (PVDF) membrane (1.4 A for 180 min in 25 mM Tris-HCl pH 8.3, 192 mM glycine). Membranes were blocked using 5% (w/v) non-fat milk or BSA (1 h/RT). Primary antibodies were incubated with membrane for 16 h at 4 °C. Developing antibodies were diluted to 0.1 µg/ml and incubated with membranes for 45 min.

2.5. Immunohistochemistry

Immunohistochemical staining was carried out by Dr Chaker Adra (Harvard Medical School) with the Large Volume DAKO LSAB2 Kit, Peroxidase (Dakopatts, Copenhagen, Denmark) according to the Manufacturer's instructions. Formalin-fixed sections were deparaffinised in xylene (5 min, three times), dehydrated in ethanol and incubated with 3% hydrogen peroxide for 15 min, with blocking solution for 60 min and with TRPA1-specific polyclonal antibody diluted 1/100 in 0.01% phosphate-buffered saline (PBS) for over night at 4 °C temperature. A section without first antibody was also carried out as a negative control. The sections were washed with Tris buffer and treated with 0.01% biotin solution for 10 min, then incubated in the biotinylated polyclonal secondary antibody for 60 min. After washing with Tris buffer, the sections were visualized with 0.03% diaminobenzidine, then counterstained with hematoxylin and mounted.

2.6. Gel electrophoresis of DNA and band excision

Standard agarose gel electrophoresis was performed using 1% agarose in TAE buffer (comprising 40 mM Tris, 20 mM Acetic acid, and 2 mM EDTA pH

8.3). Samples were loaded in a 10x sample buffer comprising Bromophenol blue (0.05% w/v), sucrose (40% w/v), EDTA (0.1 M, pH 8.0), and SDS (0.5% w/v), and electrophoresed at 9–15 V/cm for the time needed to achieve adequate resolution. Electrophoretic standards comprised a DNA or RNA ladder spanning 100 bp–10 kb range. DNA gels were visualized on a ChemiDoc system (BioRad), using Ethidium Bromide (0.5 µg/ml final). For gel purification, bands were excised using a clean scalpel blade and a DNA extraction was performed using the QIAquick Gel Extraction Kit (QIAGEN Inc., Valencia, CA 91355).

2.7. Northern Blots

Multiple tissue and immune system Northern blots were purchased from Clontech (Palo Alto, CA) and probed according to the Manufacturer's instructions. Multiple cell line Northern blots were produced using 1 µg/lane poly A⁺ mRNA. The probing of these membranes was carried out as follows. Probes were ³²P labelled using random priming. Membranes were hybridized with radio labelled probe for 2 h/65 °C. After two washes in 2 × SSC/0.05% SDS/RT for 20 min and two washes in 0.1 × SSC/0.1% SDS/50 °C for 20 min, membranes were auto-radiographed or imaged using a Cyclone Phosphorimager (Perkin Elmer, Madison, WI).

2.8. Patch-clamp experiments

Cells grown on glass coverslips were transferred to the recording chamber and kept in a standard modified Ringer's solution of the following composition (in mM): NaCl 140, KCl 2.8, CaCl₂ 1, MgCl₂ 2, glucose 10, HEPES-NaOH 10, pH 7.2, with osmolarity typically ranging from 295 to 325 mOsm. Intracellular pipette-filling solutions contained (in millimolar): Cs-glutamate 140, NaCl 8, MgCl₂ 1, Cs-BAPTA 10, HEPES-CsOH, pH 7.2 adjusted with CsOH. All chemicals used were purchased from Sigma. Patch-clamp experiments were performed in the tight-seal whole-cell configuration at 21–25 °C. High-resolution current recordings were acquired by a computer-based patch-clamp amplifier system (EPC-9, HEKA, Lambrecht, Germany). Patch pipettes had resistances between 2 and 4 MΩ after filling with the standard intracellular solution. Immediately following establishment of the whole-cell configuration, voltage ramps of 50 ms duration spanning the voltage range of –100 to +100 mV were delivered from a holding potential of 0 mV at a rate of 0.5 Hz over a period of 500 s. All voltages were corrected for a liquid junction potential of 10 mV between external and internal solutions because of glutamate use as intracellular anion. Currents were filtered at 2.9 kHz and digitized at 100 µs intervals. Capacitive currents and series resistance were determined and corrected before each voltage ramp using the automatic capacitance compensation of the EPC-9. The low-resolution temporal development of membrane currents was assessed by extracting the current amplitude at –80 mV from individual ramp current records. Where applicable, statistical errors of averaged data are given as means ± S.E.M. with n determinations.

3. Results

3.1. TRPA1 is not restricted to tissues of the CNS

TRPA1 (ANKTM1) was originally cloned from human lung fibroblasts, including the IMR-90 cell line [8]. However, in subsequent studies, an extremely limited tissue distribution for TRPA1 has been proposed [1–3]. We were able to reproduce the finding that TRPA1 transcripts are detectable in IMR-90 fibroblasts (Fig. 1A, left panel). Extremely long exposure times for multiple tissue Northern blots (Fig. 1A, right panel) suggested that TRPA1 transcripts are of low abundance but are expressed in non-sensory tissue contexts, including small intestine, colon, skeletal muscle, heart, brain, and components of the immune system. Since the presence of transcript does not necessarily imply the presence of protein, we designed an antibody to TRPA1.

Initially, we constructed a cell line with tetracycline-inducible expression of human TRPA1. In this system, TRPA1 was modified with a FLAG epitope to facilitate detection of the protein. Fig. 1A (left panel) and Fig. 1B show that tetracycline treatment of TREx-TRPA1 cells results in the induced expression of a 5 kb mRNA and a 120 kDa FLAG-tagged protein, respectively. The predicted molecular weight of unmodified human TRPA1 is 127.4 kDa. Anti-TRPA1 was raised against a C-terminal peptide epitope KMEIISSETEDDDSHCSFQDR (residues 1071–1090). Fig. 1B shows that the anti-TRPA1 and anti-FLAG antibodies reciprocally immunoprecipitate the FLAG-TRPA1 protein. Moreover, FLAG-TRPA1 is detected by anti-TRPA1 Western blots. Taken together, these data suggest that our novel anti-TRPA1 specifically recognizes both native and denatured TRPA1.

We used anti-TRPA1 to probe multiple tissue Western blots, and we noted a protein doublet of approximately 120 kDa in protein samples derived from tissues including brain, heart, small intestine, lung, skeletal muscle, and pancreas. The multiple mobility forms of TRPA1 are suggestive of extensive post-translational modification. The data in Fig. 1C suggest a wider tissue distribution for TRPA1 than noted in ([1–3]), and are consistent with original reports of non-neuronal expression for TRPA1 [8]. The expression of TRPA1 in multiple immortalized cell lines from diverse sources (Fig. 1D), and the immunohistochemistry data in Fig. 1E, argue against a neurally restricted distribution for TRPA1.

In addition to its expression in non-neuronal contexts, Jacquemar et al. suggested that TRPA1 expression is dysregulated in certain carcinomas. We surveyed 195 tumors and matched normal tissues for the expression levels of TRPA1 mRNA and protein. Significant differences between TRPA1 mRNA levels in tumor and normal samples were observed in only 1–2 cases from 148 surveyed (>2 fold net change). In contrast, a survey of TRPA1 protein levels in 47 human tumors and matched normal tissues revealed a marked association between increased TRPA1 protein and transformed phenotype (Fig. 1E). We cannot exclude that TRPA1 protein levels are dysregulated in tumor contexts because of small but significant alterations in mRNA levels. Alternatively, TRPA1 protein levels may be controlled post-translationally, through a mechanism that is sensitive to oncogenic transformation.

3.2. TRPA1 associates with the tumor suppressor gene product, CYLD

Our interaction trap analysis (not shown) of TRPA1 has provided an extensive set of potential binding partners for the TRPA1 cytoplasmic tails. We analyzed this data set for proteins that could regulate TRPA1 levels post-translationally. The CYLD gene product was isolated as a potential binding partner for the TRPA1 amino-terminal cytoplasmic tail. CYLD itself is a cytosolic de-ubiquitinating enzyme for which a limited set of substrates has been defined to date, within the TNF/NFκB pathway [17–19,42,43]. CYLD controls the ubiquitination status, and hence expression levels, of its

substrates. Interestingly, premature termination mutations within CYLD are the causative genetic defect in cylindroma cancers [21–23,25].

We sought to validate the potential interaction of TRPA1 and CYLD. The human CYLD cDNA was subcloned into a

tetracycline-inducible expression vector. An amino-terminal 6×His epitope tag was incorporated into CYLD in order to facilitate detection of the protein. Fig. 2A (left panel) shows that introduction of the His₆-CYLD cDNA, transiently, or stably, into HEK293 cells results in the production of a

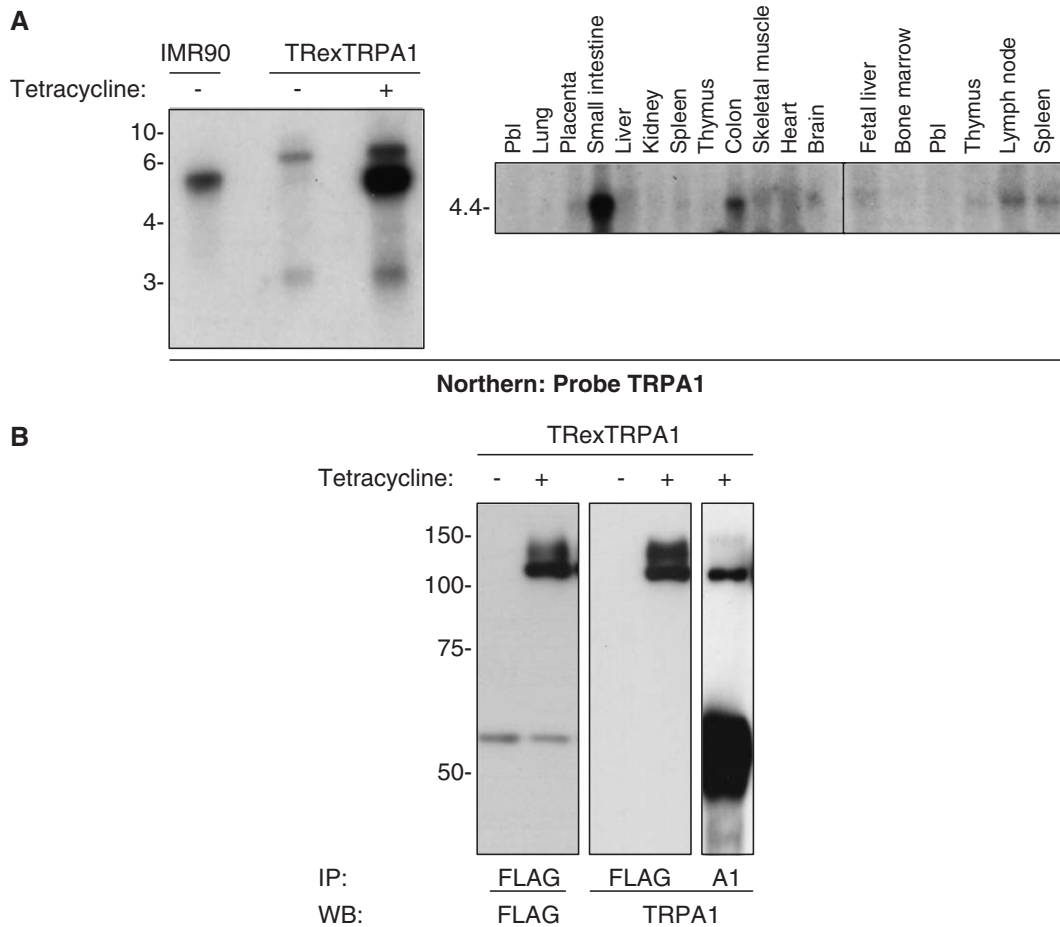


Fig. 1. TRPA1 is expressed in sensory, and non-sensory, tissue contexts. (A) Northern analysis of IMR-90 and HEK293TREx-TRPA1 cell lines, and TRPA1 tissue distribution. *Left Panel.* A Northern membrane comprising RNA-derived from IMR-90 (human lung epithelial cells) and HEK293 TRExTRPA1 cells was hybridized with ³²P labelled probe corresponding to a 617 bp EcoRV/Not1 fragment of TRPA1 cDNA. Signal was visualized using autoradiography after an 8-week exposure. RNA marker sizes are in kilobases. *Right panel.* Multiple tissue Northern membrane (Clontech, Palo Alto, CA) was hybridized with ³²P labelled probe corresponding to a 617 bp EcoRV/Not1 fragment of TRPA1 cDNA. Signal was visualized using autoradiography. RNA marker sizes are in kilobases. (B) Validation of anti-TRPA1. TREx TRPA1 cells were treated with tetracycline for 16 h (1 µg/ml). FLAG-TRPA1 protein was immunoprecipitated from cellular lysates using either 2 µg anti-FLAG or 4 µg anti-TRPA1. Immunocomplexes were resolved by 10% SDS-PAGE and the Western blotted with the indicated antibodies. (C) Expression of TRPA1 protein in human tissues. *Upper panel.* Matched human tissue protein samples were resolved using 10% SDS-PAGE and Western blotted with anti-TRPA1. *Lower panel.* Immunohistochemistry of human tissue sections using anti-TRPA1. Tissue sections were de-paraffinized and stained with the anti-TRPA1 antibody, following extensive control stainings (data not shown) to establish the correct conditions. Immunostaining was visualized using diaminobenzidine (brown coloration) and counterstained with haematoxylin/eosin (purple coloration). Clear expression of TRPA1 was detected in heart myocytes, gastrointestinal mucosa, brain, renal tubular cells, hepatocytes, pancreatic acinar cells, prostatic transitional epithelial cells. Expression was detected in the skin epidermis (including keratinocytes, melanocytes, and Langerhans' cells). (D) Cell line expression of TRPA1. Matched protein samples from various immortalized cell lines were Western blotted for the presence of TRPA1 protein. Jurkat, human T lymphocyte; Ramos, human B lymphocyte; MCF/MDA, human breast epithelia; PC12, rat pheochromocytoma; HT22, murine neuron; IMR90, human lung fibroblast; Cath/CAD, murine neuron. (E) Alteration in TRPA1 protein levels are observed in human cancers. mRNA analysis. A BD Biosciences (Palo Alto, CA, USA) human cancer profiling array II was spotted with matched amounts of total RNA derived from 154 tumour and corresponding normal tissues from patients. The membrane was hybridized using a TRPA1 cDNA probe identical to that used in the Northern analysis shown previously. TRPA1 levels were visualized using ³²P phosphor-imaging, then quantified using OptiQuant software. *Protein analysis.* A BioChain Inc (Hayward, CA) human cancer expression array was blocked and then hybridized, using anti-TRPA1 (0.5 µg/ml) under the same Western blotting conditions that have yielded specific signals in total cellular lysates, and control probeds were performed to exclude differential hybridization of the secondary antibody. TRPA1 levels were visualized using ECL, and then quantified using OptiQuant software. Global background subtraction was performed and data were converted to fold differences between tumor and normal samples (horizontal line indicates one-fold, i.e. no significant difference between samples). Tukey plots of data ranges for both mRNA and protein arrays indicate that protein, but not mRNA levels, for TRPA1 tend to be altered in tumor samples relative to matched normal samples. Median is indicated by ▲, first and third quartiles by ◆, minimum and maximum by ●.

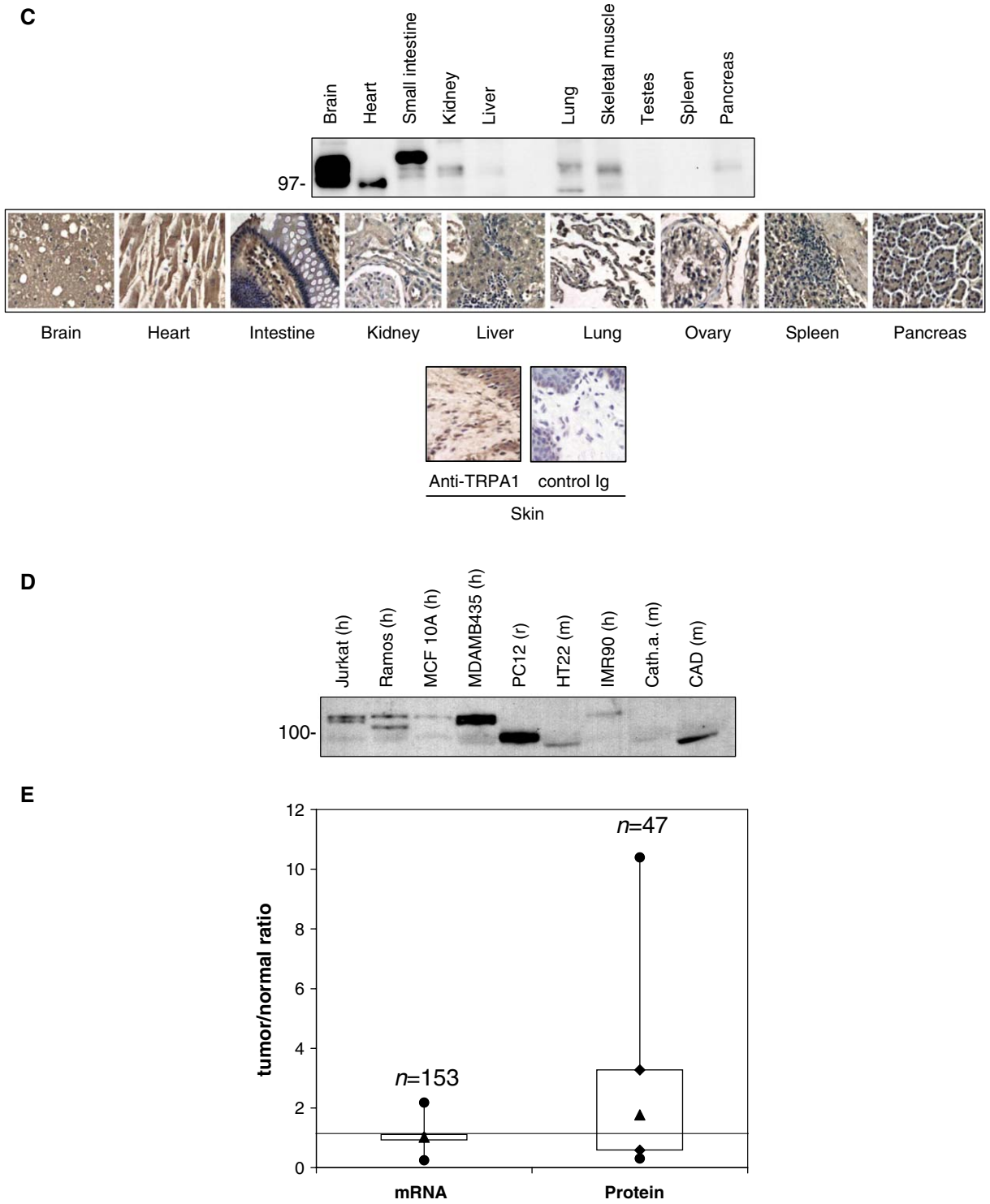


Fig. 1 (continued).

107 kDa protein that corresponds to His₆-CYLD. We performed co-immunoprecipitations to test whether CYLD and TRPA1 are associated in a physiological complex. TREx-TRPA1 cells were transiently transfected with His₆-CYLD. Fig. 2A (right panel) shows that anti-His immunocomplexes isolated from these cells contain FLAG-TRPA1. Fig. 2B shows that over-expressed CYLD interacts with endogenous

TRPA1. We also explored the potential for TRPA1 to interact with CYLD in a native TRPA1 expression context. The Jurkat T cell line expresses both TRPA1 and CYLD (Figs. 1D and 2C). Anti-CYLD immunoprecipitates from this cell line contain TRPA1 protein (Fig. 2D). Taken together, these data suggest that TRPA1 and CYLD can interact in a physiological complex.

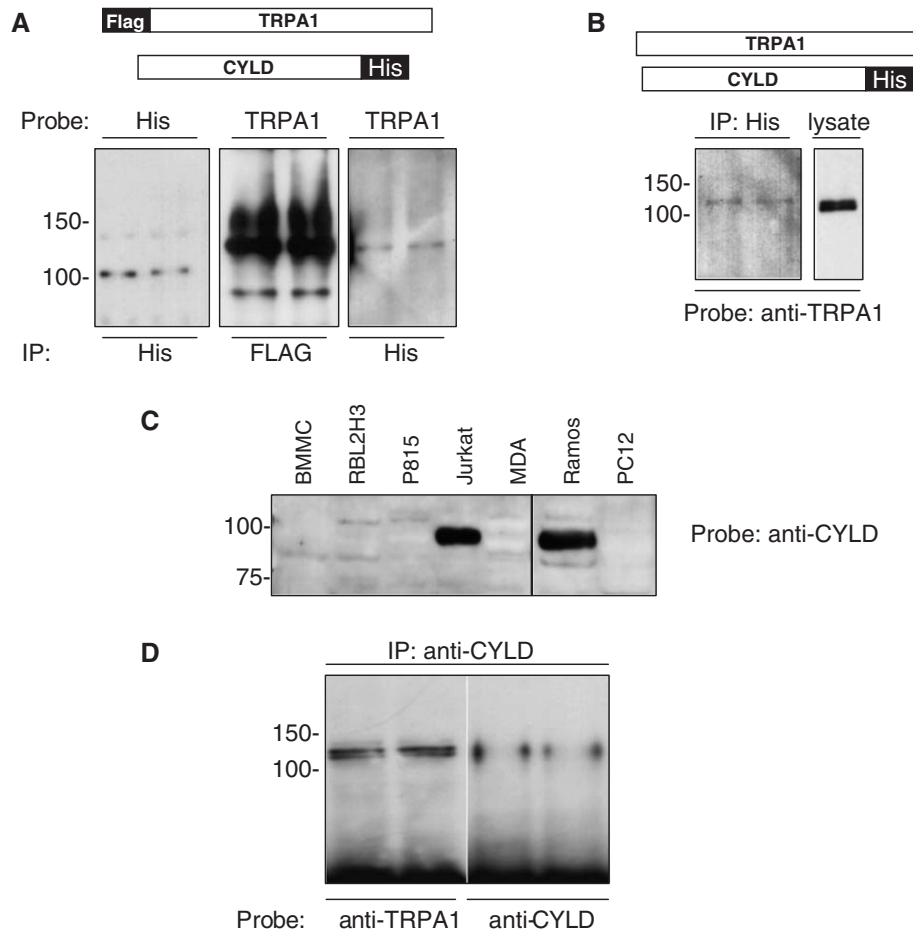


Fig. 2. (A) Co-immunoprecipitation of co-expressed TRPA1 and CYLD. *Left panel.* Introduction of the His₆-CYLD cDNA into HEK293 cells results in production of a 107 kDa protein that corresponds to His₆-CYLD. *Center and right panels.* Anti-His immunocomplexes isolated from these cells contain FLAG-TRPA1. HEK293T_{REx}TRPA1 cells (bearing FLAG-TRPA1 constructs) were re-transfected with His₆-CYLD construct. After 72 h for protein expression, cells were lysed and immunoprecipitated with 2 μg of the indicated antibody. Samples were resolved by 10% SDS-PAGE and Western-blotted using either anti-His or anti-TRPA1 antibodies. (B) His₆-CYLD interacts with endogenous TRPA1. MDAMB435 cells were transiently re-transfected with the His₆-CYLD construct. These cells were selected for their high endogenous expression levels for TRPA1. After 72 h for protein expression, cells were either lysed and immunoprecipitated with 2 μg of the anti-His antibody, or acetone-precipitated to recover total protein. Samples were resolved by 10% SDS-PAGE and Western-blotted using anti-TRPA1 antibody. (C) Co-immunoprecipitation of endogenous CYLD and TRPA1. *Upper panel.* Western blotting of cellular lysates with anti-CYLD established that Jurkat T cell express significant amounts of CYLD protein, and demonstrates the specificity of the anti-CYLD antibody. *Lower panel.* Anti-CYLD immunocomplexes isolated from Jurkat T cells contain TRPA1 protein. Immunocomplexes were resolved on duplicate 10% SDS-PAGE and probed with either anti-TRPA1 or anti-CYLD.

3.3. TRPA1 is a substrate for de-ubiquitination by CYLD

The interaction between CYLD and TRPA1 suggests: (1) that CYLD may have substrates that lie outside the TNF/NF κ B pathway, and (2) that TRPA1 expression levels may be controlled by a ubiquitination mechanism that involves CYLD. We assayed the total complement of ubiquitin-containing proteins in HEK293 cells in which His₆-CYLD was transiently over-expressed. Fig. 3A shows that His₆-CYLD over-expression results in a decrease in the total ubiquitin content of HEK cellular proteins. Control cells, or those transfected with an irrelevant cDNA, did not display this decrease in protein ubiquitinylation. These data establish that the heterologously expressed CYLD protein is active as a ubiquitin hydrolase. Fig. 3A also implies that, at least under over-expression conditions, CYLD has numerous cellular substrates.

We asked if TRPA1 is ubiquitinylated. Fig. 3B shows that immunoprecipitated FLAG-TRPA1 may be visualized in an anti-ubiquitin Western blot, suggesting that a population of TRPA1 protein is ubiquitinylated in resting cells. Treatment with the proteasome inhibitor, lovastatin, leads to a marked increase in the levels of the multi-ubiquitinylated (high molecular weight) forms of TRPA1 in resting cells (data not shown). These data suggest that proteolysis, via ubiquitin targeting to the proteasome, is a determinant of the basal turnover of TRPA1 protein.

We used the TRPA1 ligand, icilin, to ask if the ubiquitinylation of TRPA1 is modified following activation of the channel [1,3]. Fig. 3C shows that, in our T_{REx}TRPA1 cells, icilin application results in the presence of a slightly outwardly-rectifying conductance that is not present in control cells. T_{REx}TRPA1 cells are refractory to repeated applications of icilin. Icilin application is followed by a marked increase in the

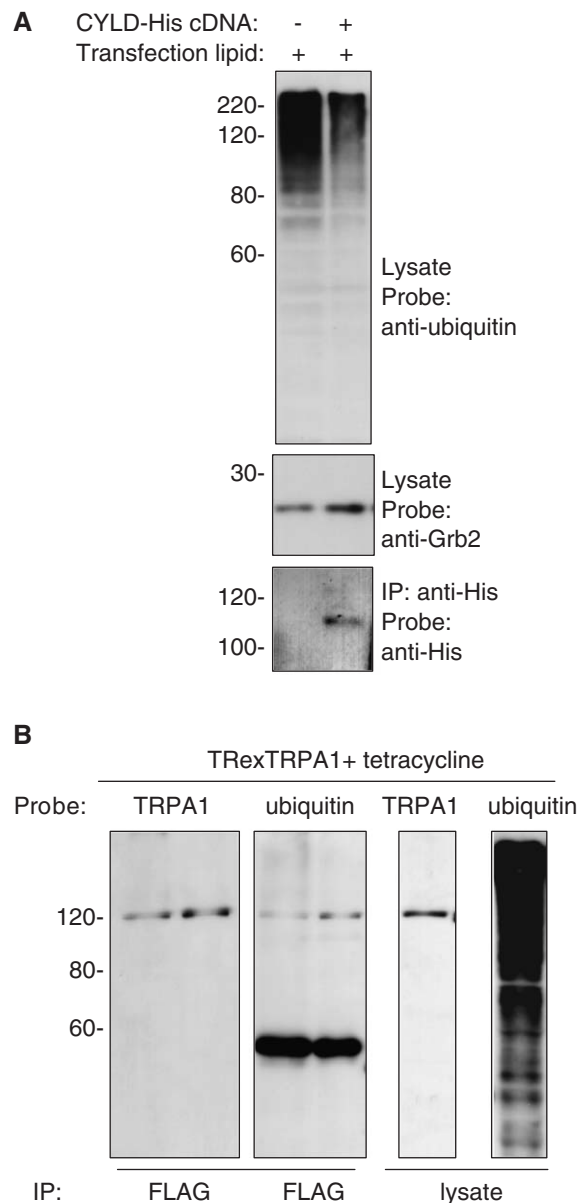


Fig. 3. (A) His₆-CYLD over-expression results in a decrease in the total ubiquitin content of HEK cellular proteins. HEK293 cells were transiently transfected with the His₆-CYLD construct. After 72 h for protein expression, cell lysates were produced and normalized for total protein levels using a Bradford assay. *Top panel*. Lysates were acetone-precipitated to recover total protein, resolved by 10% SDS-PAGE, and Western-blotted to reveal ubiquitinated proteins. *Center panel*. Probing control with anti-Grb2 antibody indicates that a decrease in ubiquitinated protein levels is not a loading artefact on the Western blot. *Lower panel*. Lysates were immunoprecipitated using 2 µg of the anti-His antibody, in order to confirm the transfected expression of the His₆-CYLD protein. (B) TRPA1 is a ubiquitinated protein. TRexTRPA1 cells were treated with 1 µg/ml tetracycline for 16 h at 37 °C. Cell lysates were prepared and immunoprecipitated with 2 µg anti-FLAG, or acetone-precipitated to recover total protein. Duplicate Western blots were then probed using either anti-TRPA1 or anti-ubiquitin antibodies. (C) TRPA1 conductance is activated by icilin in TRexTRPA1 cells. TRexTRPA1 cells were treated with tetracycline (1 µg/ml) for 16 h at 37 °C. TRPA1 currents were measured in the whole-cell patch-clamp configuration under the solution conditions described in Methods. Icilin (12.5 µM) was applied using a wide-tipped perfusion pipette for the time-periods that are indicated by the black bars. *Left panel*. Time-resolved current recording. *Right panel*. Current/voltage relationship for TRPA1 conductance that is activated following icilin perfusion. (D) Icilin application increases in the number of multi-ubiquitinated forms of TRPA1. TRexTRPA1 cells were treated with tetracycline (1 µg/ml) for 16 h at 37 °C. Cells were resuspended in Ringer buffer supplemented with 1 mM CaCl₂ and treated with vehicle, or icilin (12.5 µM) for 10 min at 37 °C. Reactions were stopped by quenching with cold PBS and lysis on ice. Cell lysates were immunoprecipitated using 2 µg anti-FLAG and resolved by 10% SDS-PAGE. Duplicate Western blots were probed using either anti-FLAG or anti-ubiquitin antibodies. (E) Over-expression of CYLD suppresses the icilin-induced ubiquitinylation of TRPA1. TRexTRPA1 cells were transiently re-transfected with His₆-CYLD, or with a control plasmid using the TransIT lipid transfection reagent. Cells were treated with tetracycline (1 µg/ml), or vehicle, for 16 h at 37 °C. Cells were resuspended in Ringer buffer supplemented with 1 mM CaCl₂ and treated with vehicle, or icilin (12.5 µM) for 10 min at 37 °C. Reactions were stopped by quenching with cold PBS and lysis on ice. Cell lysates were immunoprecipitated using 2 µg anti-FLAG and resolved by 10% SDS-PAGE. Duplicate Western blots were probed using either anti-TRPA1 or anti-ubiquitin antibodies. (F) Ligand-induced dissociation of the TRPA1-CYLD protein complex. Anti-CYLD was used to capture immunocomplexes from vehicle or icilin-treated Jurkat T cells. Immunocomplexes were resolved on duplicate 10% SDS-PAGE and Western blotted for the presence of TRPA1 and CYLD. After ligand application there is a decrease in the degree of association between TRPA1 and the de-ubiquitinating enzyme CYLD.

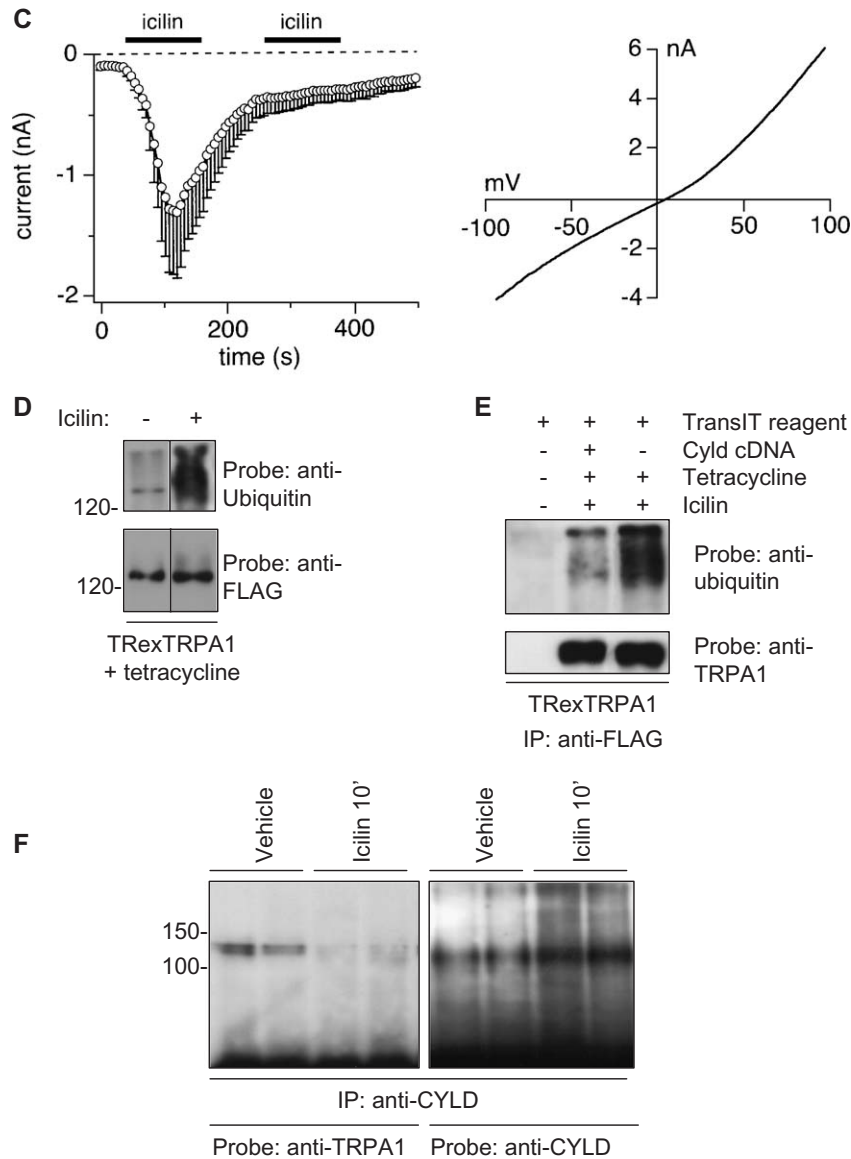


Fig. 3 (continued).

number of multi-ubiquitylated forms of TRPA1 (Fig. 3D). We also observe that over-expression of CYLD suppresses the icilin-induced ubiquitinylation of TRPA1 (Fig. 3E). These data suggest that regulated ubiquitinylation follows ligand application to TRPA1. Moreover, we propose that CYLD participates in the control of TRPA1 protein levels through an interaction with the channel.

Fig. 3F suggests that the interaction between TRPA1 and CYLD is dynamic, and depends upon the activation status of TRPA1. Jurkat cells were used in this experiment, because they are a native context for both TRPA1 protein and CYLD. Immunoprecipitation of CYLD was performed in lysates that were derived from vehicle, or icilin, treated cells. After icilin treatment, the levels of TRPA1 in the anti-CYLD immunocomplexes appeared markedly reduced. These data imply that, following ligand binding, the channel protein loses its interaction with the de-ubiquitinating enzyme. This event may

be a permissive step for the subsequent increase in ubiquitinylation of TRPA1 that we observe after ligand exposure.

3.4. CYLD over-expression dys-regulates TRPA1 protein levels

We asked whether the cellular concentration of the CYLD enzyme has any bearing upon the levels of TRPA1 protein. We compared the levels of TRPA1 protein that could be immunoprecipitated from TRexTRPA1 cells that were re-transfected for 48 h with either vector, or a His₆-CYLD construct (Fig. 4A). Protein samples were matched using a Lowry Assay, and this matching is shown in the lower panel of Fig. 4A. The upper panel of this Figure shows that TRPA1 levels appear increased in the presence of CYLD over-expression, compared to vector-transfected control cells. Fig. 4B shows the level of His₆-CYLD that was expressed during this transfection experiment. These findings indicate that over-

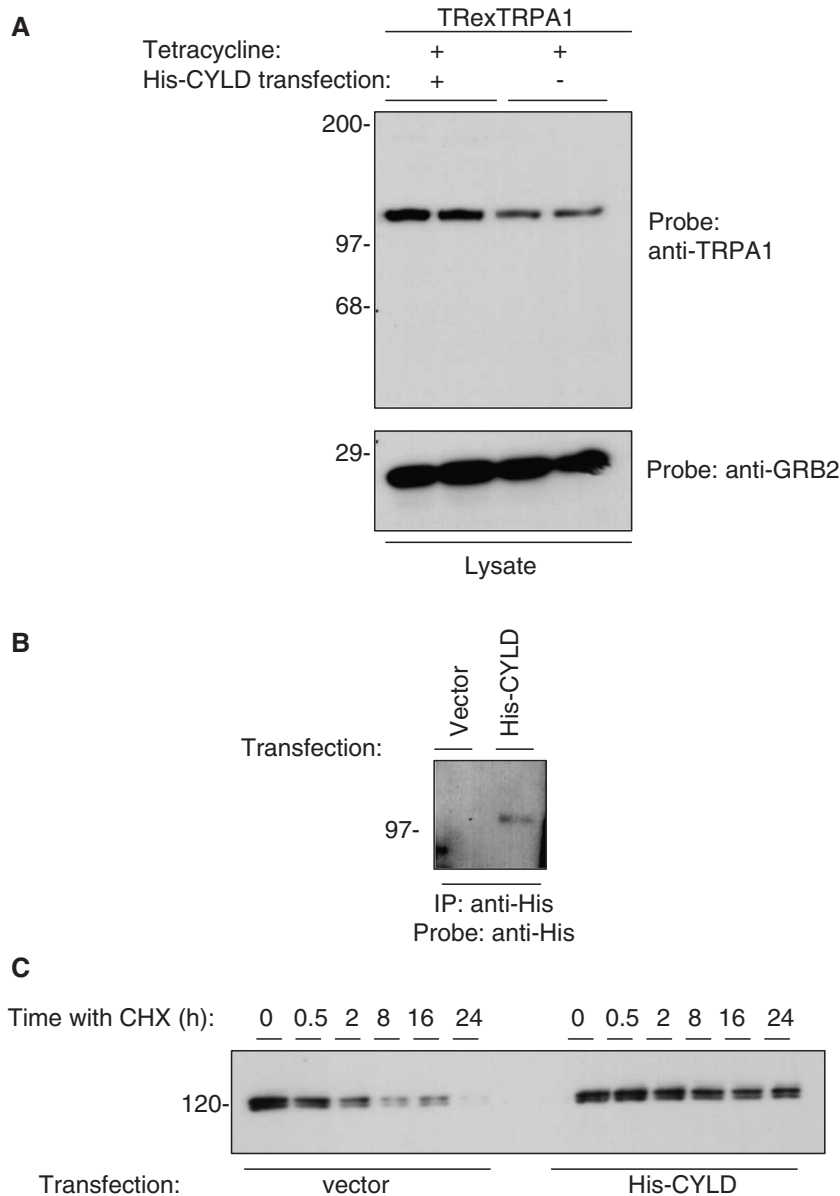


Fig. 4. (A) CYLD over-expressing cells contain more TRPA1 than control transfectants. HEK293TRexTRPA1 cells were transiently re-transfected with His₆-CYLD or with a control plasmid using the TransIT lipid transfection reagent. Cells were treated with tetracycline (1 μ g/ml) for 16 h at 37 °C. Cell lysates were prepared and normalized using a Lowry assay. Protein was recovered by acetone-precipitation and resolved by 10% SDS-PAGE. After electrotransfer, membranes were divided and probed with anti-TRPA1 (*top panel*) or anti-Grb2 (*lower panel*, presented as a loading control). (B) Expression of CYLD in transiently re-transfected cells. Cell lysates were immunoprecipitated using 2 μ g anti-His and resolved by 10% SDS-PAGE. Western blot was probed using anti-His to confirm expression of His₆-CYLD protein in the experiment presented in Fig. 4A. (C) Transfection of HEK293 cells with His₆-CYLD protects TRPA1 protein levels. HEK293 cells were transfected with either control plasmid or pcDNA5T/O His₆-CYLD. After 24 h in culture, cycloheximide (20 μ g/ml) was added to prevent further protein synthesis and protein samples were harvested at the indicated times. Protein levels were normalized between samples and loaded onto 10% SDS-PAGE gels that were subsequently Western-blotted for TRPA1 levels.

expressed TRPA1 is apparently sensitive to the presence of excess CYLD. We asked whether endogenous TRPA1 protein levels were similarly sensitive to the presence of CYLD protein. HEK293 cells were transfected for 18 h with either vector, or His₆-CYLD construct. These cells were exposed to either vehicle, or the protein translation inhibitor cycloheximide (20 μ g/ml) for the indicated times. In the presence of cycloheximide, total protein levels, and the levels of TRPA1 (left panel, Fig. 4C), decline in the absence of de novo protein synthesis. This decline is presumed to reflect the basal turnover of TRPA1.

Fig. 4B (right panel) shows that the presence of over-expressed His₆-CYLD slows the decline in TRPA1 levels, indicating that the over-expression of the de-ubiquitinating enzyme CYLD tends to protect TRPA1 from basal turnover.

4. Discussion

Calcium signalling is connected to various aspects of ordered growth control and cellular differentiation. It is therefore unsurprising that emergent evidence suggests that expression

levels of various calcium channels are altered in some oncogenically transformed cells. Alterations in the levels of TRPs and other channels have been shown to correlate with both oncogenic potential and the transition to a metastatic state [44–53]. Alterations in TRPA1 levels would be predicted to have calcium-dependent functional consequences for the cell, in the presence of an appropriate endogenous activating signal (e.g. GPCR ligands [1,5,7]). We have described that increases in TRPA1 protein levels tend to associate with a transformed phenotype in the tumors surveyed here. Future experiments will determine whether TRPA1 dys-regulation is a primary cause, or secondary consequence, of transformation events. Depending on the outcome of these studies, TRPA1 may be of interest as a diagnostic marker for certain transformations, or as a possible target for interference with the transformation process.

The present data show that TRPA1 is a substrate for the cellular ubiquitination machinery. Modulation of TRPA1 ubiquitination status clearly has the potential to control the lifetime of TRPA1 protein, and may contribute to the observable differences in TRPA1 protein levels across different stages in development, tissue differentiation, or under conditions of oncogenic transformation ([8,9] and HT/AJS unpublished data). Here, an analogy can be drawn with the regulatory mechanisms that control the levels of Aquaporin-1, one of the few ion channels with a previously studied ubiquitination pathway. In the case of Aqp-1, exposure to long term hypotonic stress causes decreased ubiquitination of the channel and a resultant increase in protein levels [36]. While our data suggest that TRPA1 levels are acutely down-regulated following ligand exposure, we have not discerned the effects of chronic exposure to TRPA1 ligands upon protein expression levels. Future work will be required to determine the relative contributions of controlled ubiquitination and transcriptional/translational mechanisms to the control of TRPA1 protein levels under both normal and disease conditions.

In addition to a potential role in determining basal expression levels of the TRPA1 channel, our data suggest that the ubiquitination module participates in control of TRPA1 over more acute time-courses. Ubiquitination of TRPA1 is apparently increased following ligand binding to the TRPA1 channel. This coincides with, and probably depends upon, dissociation of the de-ubiquitinating enzyme CYLD from its interaction with TRPA1. The enhanced ubiquitination that is permitted following CYLD dissociation may be a component of the signal termination mechanism for TRPA1, although our current experiments are limited to small molecule activators of TRPA1 (icilin and cannabinoid compounds). Future work will determine whether temperature-evoked activation of TRPA1 is followed by a similar series of events. Moreover, the fate of ubiquitinated TRPA1 may not be inevitable degradation, since transient ubiquitination and de-ubiquitination have been shown to precede recycling of the plasma membrane for some membrane proteins [13,14,30].

The CYLD protein is a ubiquitin hydrolase, one of an extensive family of de-ubiquitinating enzymes (DUBs) [16]. It is not yet clear whether any related DUB enzymes have activity at TRPA1, or whether CYLD targets other members of the TRP

family. To date, targets for CYLD have been described only within the TNF signaling pathway [17–19,42]. Here, de-ubiquitination by CYLD has been described to control the lifetime of proteins that are involved in TNF signaling, and hence to modulate cellular sensitivity and functional responses to TNF-receptor ligands. Our data suggest that, at least in an over-expression system, CYLD may have numerous potential targets, including TRPA1. In light of the possibility that CYLD is a potential control point for regulation of TRPA1 levels, it will be interesting to explore how the newly defined phosphorylation pathways that modify CYLD activity [20] affect TRPA1.

CYLD is of interest since familial mutations in the *CYLD* gene lead to the development of a particular class of cancers, the cylindromas (turban tumor syndrome). Heritable mutations in *CYLD* have also been described in adenoid cystic carcinomas and tricho-epitheliomas [22–25,54]. These classes of cancers are all typically benign and originate in adnexal structures surrounding the sebaceous or salivary glands. The pathology-associated mutations in *CYLD* that have been described occur in the 3' coding region of *CYLD* and lead to premature termination of the protein [21,22,24,27]. This termination is accompanied by loss of activity as an ubiquitin hydrolase. The development of these cancers is currently attributed to a defect in, or dys-regulation of, TNF signaling that results from inefficient de-ubiquitination of CYLD substrates within the TNF pathway [17,18,42,55]. Defective TNF signaling results in a direct effect upon pro-apoptotic pathways and hence ordered growth and proliferation. Since no such clear linkage is known between TRPA1 signaling and cellular transformation, it is not yet clear whether dys-regulation of TRPA1 levels may be a causal event in the development of cylindromas and related cancers. However, our data do suggest that oncogenic mutations in *CYLD* would be predicted to alter cellular levels of TRPA1, which may be of relevance to the development of diagnostic assays.

Acknowledgements

This work was supported by the Leahi Fund for Pulmonary Research and NIH 2P20 R016467-04 (grants to H.T.). The authors thank Linden Doescher and Cora Speck for technical assistance and manuscript preparation.

References

- [1] M. Bandell, G.M. Story, S.W. Hwang, V. Viswanath, S.R. Eid, M.J. Petrus, T.J. Earley, A. Patapoutian, *Neuron* 41 (6) (2004) 849.
- [2] D.M. Bautista, P. Movahed, A. Hinman, H.E. Axelsson, O. Sterner, E.D. Hogestatt, D. Julius, S.E. Jordt, P.M. Zygmunt, *Proc. Natl. Acad. Sci. U. S. A.* 102 (34) (2005) 12248.
- [3] G.M. Story, A.M. Peier, A.J. Reeve, S.R. Eid, J. Mosbacher, T.R. Hricik, T. J. Earley, A.C. Hergarden, D.A. Andersson, S.W. Hwang, P. McIntyre, T. Jegla, S. Bevan, A. Patapoutian, *Cell* 112 (6) (2003) 819.
- [4] K. Obata, H. Katsura, T. Mizushima, H. Yamanaka, K. Kobayashi, Y. Dai, T. Fukuoka, A. Tokunaga, M. Tominaga, K. Noguchi, *J. Clin. Invest.* 115 (9) (2005) 2393.
- [5] B. Namer, F. Seifert, H.O. Handwerker, C. Maihofner, *Neuroreport* 16 (9) (2005) 955.

- [6] D.P. Corey, J. Garcia-Anoveros, J.R. Holt, K.Y. Kwan, S.Y. Lin, M.A. Vollrath, A. Amalfitano, E.L. Cheung, B.H. Derfler, A. Duggan, G.S. Geleoc, P.A. Gray, M.P. Hoffman, H.L. Rehm, D. Tamasauskas, D.S. Zhang, *Nature* 432 (7018) (2004) 723.
- [7] S.E. Jordt, D.M. Bautista, H.H. Chuang, D.D. McKemy, P.M. Zygmunt, E. D. Hogestatt, I.D. Meng, D. Julius, *Nature* 427 (6971) (2004) 260.
- [8] D. Jaquemar, T. Schenker, B. Trueb, *J. Biol. Chem.* 274 (11) (1999) 7325.
- [9] T. Schenker, B. Trueb, *Exp. Cell Res.* 239 (1) (1998) 161.
- [10] A. Mani, E.P. Gelmann, *J. Clin. Oncol.* 23 (21) (2005) 4776.
- [11] D.E. Goll, V.F. Thompson, H. Li, W. Wei, *Cong. J. Physiol. Rev.* 83 (3) (2003) 731.
- [12] V. Stoka, B. Turk, V. Turk, *IUBMB Life* 57 (4–5) (2005) 347.
- [13] K.H. Baek, *Exp. Mol. Med.* 35 (1) (2003) 1.
- [14] L. Hicke, *Trends Cell Biol.* 9 (3) (1999) 107.
- [15] R.L. Welchman, C. Gordon, R.J. Mayer, *Nat. Rev., Mol. Cell Biol.* 6 (8) (2005) 599.
- [16] C.A. Semple, *Genome Res.* 13 (6B) (2003) 1389.
- [17] E. Trompouki, E. Hatzivassiliou, T. Tschritzis, H. Farmer, A. Ashworth, G. Mosialos, *Nature* 424 (6950) (2003) 793.
- [18] A. Kovalenko, C. Chable-Bessia, G. Cantarella, A. Israel, D. Wallach, G. Courtois, *Nature* 424 (6950) (2003) 801.
- [19] W. Reiley, M. Zhang, S.C. Sun, *J. Biol. Chem.* 279 (53) (2004) 55161.
- [20] W. Reiley, M. Zhang, X. Wu, E. Granger, S.C. Sun, *Mol. Cell Biol.* 25 (10) (2005) 3886.
- [21] G.R. Bignell, W. Warren, S. Seal, M. Takahashi, E. Rapley, R. Barfoot, H. Green, C. Brown, P.J. Biggs, S.R. Lakhani, C. Jones, J. Hansen, E. Blair, B. Hofmann, R. Siebert, G. Turner, D.G. Evans, C. Schrandt-Stumpel, F. A. Beemer, A. van Den Ouweland, D. Halley, B. Delpech, M.G. Cleveland, I. Leigh, J. Leisti, S. Rasmussen, *Nat. Genet.* 25 (2) (2000) 160.
- [22] S. Bowen, M. Gill, D.A. Lee, G. Fisher, R.G. Geronemus, M.E. Vazquez, J.T. Celebi, *J. Invest. Dermatol.* 124 (5) (2005) 919.
- [23] G. Hu, M. Onder, M. Gill, B. Aksakal, M. Oztas, M.A. Gurer, J.T. Celebi, *J. Invest. Dermatol.* 121 (4) (2003) 732.
- [24] P. Poblete Gutierrez, T. Eggermann, D. Holler, F.K. Jugert, T. Beermann, E.I. Grussendorf-Conen, K. Zerres, H.F. Merk, J. Frank, *J. Invest. Dermatol.* 119 (2) (2002) 527.
- [25] X.J. Zhang, Y.H. Liang, P.P. He, S. Yang, H.Y. Wang, J.J. Chen, W.T. Yuan, S.J. Xu, Y. Cui, W. Huang, *J. Invest. Dermatol.* 122 (3) (2004) 658.
- [26] A. Salhi, D. Bornholdt, F. Oeffner, S. Malik, E. Heid, R. Happle, K.H. Grzeschik, *Cancer Res.* 64 (15) (2004) 5113.
- [27] M. Takahashi, E. Rapley, P.J. Biggs, S.R. Lakhani, D. Cooke, J. Hansen, E. Blair, B. Hofmann, R. Siebert, G. Turner, D.G. Evans, C. Schrandt-Stumpel, F.A. Beemer, W.A. van Vloten, M.H. Breuning, A. van den Ouweland, D. Halley, B. Delpech, M. Cleveland, I. Leigh, P. Chapman, J. Burn, D. Hohl, J.P. Gorog, S. Seal, J. Mangion, *Hum. Genet.* 106 (1) (2000) 58.
- [28] K.D. Wilkinson, *J. Nutr.* 129 (11) (1999) 1933.
- [29] S. Lipkowitz, *Breast Cancer Res.* 5 (1) (2003) 8.
- [30] K. Haglund, P.P. Di Fiore, I. Dikic, *Trends Biochem. Sci.* 28 (11) (2003) 598.
- [31] G.J. Strous, C.A. dos Santos, J. Gent, R. Govers, M. Sachse, J. Schantl, P. van Kerkhof, *Curr. Top. Microbiol. Immunol.* 286 (2004) 81.
- [32] C. Geisler, *Crit. Rev. Immunol.* 24 (1) (2004) 67.
- [33] Y.C. Liu, *Annu. Rev. Immunol.* 22 (2004) 81.
- [34] R. Paolini, R. Molfetta, L.O. Beitz, J. Zhang, A.M. Scharenberg, M. Piccoli, L. Frati, R. Siraganian, A. Santoni, *J. Biol. Chem.* 277 (40) (2002) 36940.
- [35] R. Govers, T. ten Broeke, P. van Kerkhof, A.L. Schwartz, G.J. Strous, *EMBO J.* 18 (1) (1999) 28.
- [36] V. Leitch, P. Agre, L.S. King, *Proc. Natl. Acad. Sci. U. S. A.* 98 (5) (2001) 2894.
- [37] E. Gunnarson, M. Zelenina, A. Aperia, *Neuroscience* 129 (4) (2004) 947.
- [38] H. Abriel, J. Loffing, J.F. Rebhun, J.H. Pratt, L. Schild, J.D. Horisberger, D. Rotin, O. Staub, *J. Clin. Invest* 103 (5) (1999) 667.
- [39] D. Rotin, V. Kanelis, L. Schild, *Am. J. Physiol., Renal. Physiol.* 281 (3) (2001) F391.
- [40] O. Staub, H. Abriel, P. Plant, T. Ishikawa, V. Kanelis, R. Saleki, J.D. Horisberger, L. Schild, D. Rotin, *Kidney Int.* 57 (3) (2000) 809.
- [41] M.X. van Bemmelen, J.S. Rougier, B. Gavillet, F. Apotheloz, D. Daidie, M. Tateyama, I. Rivolta, M.A. Thomas, R.S. Kass, O. Staub, H. Abriel, *Circ. Res.* 95 (3) (2004) 284.
- [42] A. Regamey, D. Hohl, J.W. Liu, T. Roger, P. Kogerman, R. Toftgard, M. Huber, *J. Exp. Med.* 198 (12) (2003) 1959.
- [43] K. Saito, T. Kigawa, S. Koshiba, K. Sato, Y. Matsuo, A. Sakamoto, T. Takagi, M. Shirouzu, T. Yabuki, E. Nunokawa, E. Seki, T. Matsuda, M. Aoki, Y. Miyata, N. Hirakawa, M. Inoue, T. Terada, T. Nagase, R. Kikuno, M. Nakayama, O. Ohara, A. Tanaka, S. Yokoyama, *Structure (Camb)* 12 (9) (2004) 1719.
- [44] L.M. Duncan, J. Deeds, J. Hunter, J. Shao, L.M. Holmgren, E.A. Woolf, R. I. Tepper, A.W. Shyjan, *Cancer Res.* 58 (7) (1998) 1515.
- [45] A.J. Miller, J. Du, S. Rowan, C.L. Hershey, H.R. Widlund, D.E. Fisher, *Cancer Res.* 64 (2) (2004) 509.
- [46] B. Nilius, T. Voets, J. Peters, *Sci. STKE* 2005 (295) (2005) re8.
- [47] S. McNulty, E. Fonfria, *Pflugers Arch.* 451 (1) (2005) 235.
- [48] S.P. Fraser, J.K. Diss, A.M. Chioni, M.E. Mycielska, H. Pan, R.F. Yamaci, F. Pani, Z. Siwy, M. Krasowska, Z. Grzywna, W.J. Brackenbury, D. Theodorou, M. Koyuturk, H. Kaya, E. Battaloglu, M.T. De Bella, M.J. Slade, R. Tolhurst, C. Palmieri, J. Jiang, D.S. Latchman, R.C. Coombes, M.B. Djamgoz, *Clin. Cancer Res.* 11 (15) (2005) 5381.
- [49] E.S. Bennett, B.A. Smith, J.M. Harper, *Pflugers Arch.* 447 (6) (2004) 908.
- [50] G. Bidaux, M. Roudbaraki, C. Merle, A. Crepin, P. Delcourt, C. Slomianny, S. Thebault, J.L. Bonnal, M. Benahmed, F. Cabon, B. Mauroy, N. Prevarskaya, *Endocr. Relat. Cancer.* 12 (2) (2005) 367.
- [51] T. Fixemer, U. Wissenbach, V. Flockerzi, H. Bonkhoff, *Oncogene* 22 (49) (2003) 7858.
- [52] L. Tsavaler, M.H. Shaper, S. Morkowski, R. Laus, *Cancer Res.* 61 (9) (2001) 3760.
- [53] D. Prawitt, T. Enklaar, G. Klemm, B. Gartner, C. Spangenberg, A. Winterpacht, M. Higgins, J. Pelletier, B. Zabel, *Hum. Mol. Genet.* 9 (2) (2000) 203.
- [54] H.R. Choi, J.G. Batsakis, D.L. Callender, V.G. Prieto, M.A. Luna, A.K. El-Naggar, *Am. J. Surg. Pathol.* 26 (6) (2002) 778.
- [55] K.D. Wilkinson, *Nature* 424 (6950) (2003) 738.